Three-Dimensional Thermal Hydraulic Transient Analysis for Pump Failure in Innovative Small Sodium-Cooled Fast Reactor

Keita Endo[a*], Takashi Abe[a], Kazuhiro Fujimata[a], Hirotaka Nakahara[a]
[a]Hitachi-GE Nuclear Energy, Ltd., Hitachi-Shi, Japan

Abstract: Hitachi-GE has been developing a small sodium-cooled fast reactor (SFR) with metallic fuel to address future challenges in nuclear power. During normal operation, the heat generated in the core is cooled through primary sodium coolant circulation by electromagnetic (EM) pumps, and this heat is transferred to secondary sodium coolant via intermediate heat exchangers (IHX). In the event of a loss of these functions, the reactor is designed to be safely cooled through natural circulation of sodium and heat removal by reactor vessel auxiliary cooling system (RVACS). However, in the event of a primary EM pump failure, which is a representative design basis accident (DBA) for SFRs, there is a possibility of backflow of the primary sodium through the failed pump. Additionally, the EM pump power failure is set as the first signal to detect the failure, but the second signal is needed to account for the potential failure of the first signal to trigger a reactor scram. Therefore, this study evaluated the behavior of sodium and the effects on RVACS performance in the event of the EM pump failure using a three-dimensional thermal-hydraulic analysis. The analysis results showed that the primary sodium flowed back, increasing core outlet temperature to a maximum of 520^{o}C along with a decrease in core mass flow rate. However, natural circulation of sodium was achieved through reactor scram and the trip of the remaining EM pumps, without affecting RVACS performance. Furthermore, the results of an open-loop analysis without reactor scram showed that the increase in core outlet temperature was limited to a maximum of 508^{o}C, indicating that EM pump outlet pressure, not core outlet temperature was found to be the preferred second signal for detecting the EM pump failure.

Keywords: Sodium-cooled Fast Reactor, Heat Removal, RVACS, Natural Circulation, CFD, STAR-CCM+

1. INTRODUCTION

1.1. Background

Hitachi-GE has been developing a small SFR with metallic fuel to address future challenges in nuclear power, such as maximizing resource use and minimizing radioactive waste. PRISM [1] is an example of this type of reactor, featuring a metallic fuel core, two IHXs, and four EM pumps inside the reactor vessel (RV). During normal operation, the heat generated in the core is cooled through primary sodium coolant circulation by the EM pumps, and this heat is transferred to secondary sodium coolant via the IHXs. This reactor incorporates passive safety features for reactivity control and heat removal, which are required as safety functions. The former involves the inherent safety of metallic fuel, which helps core power to reduce steadily by giving negative reactivity due to its high thermal conductivity and expansion rate. The latter involves the RVACS, which removes heat from the outside of the guard vessel (GV) through natural circulation of air without a power supply and human intervention. Figure 1 shows a schematic of RVACS. In this system, outside air is drawn in from the stack and flows around the outside of the GV. Finally, the warmed air is exhausted from the stack. The collector cylinder functions to separates the descending and ascending airflow, insulating the outside of the descending airflow side to suppress radiation heat transfer to the air.

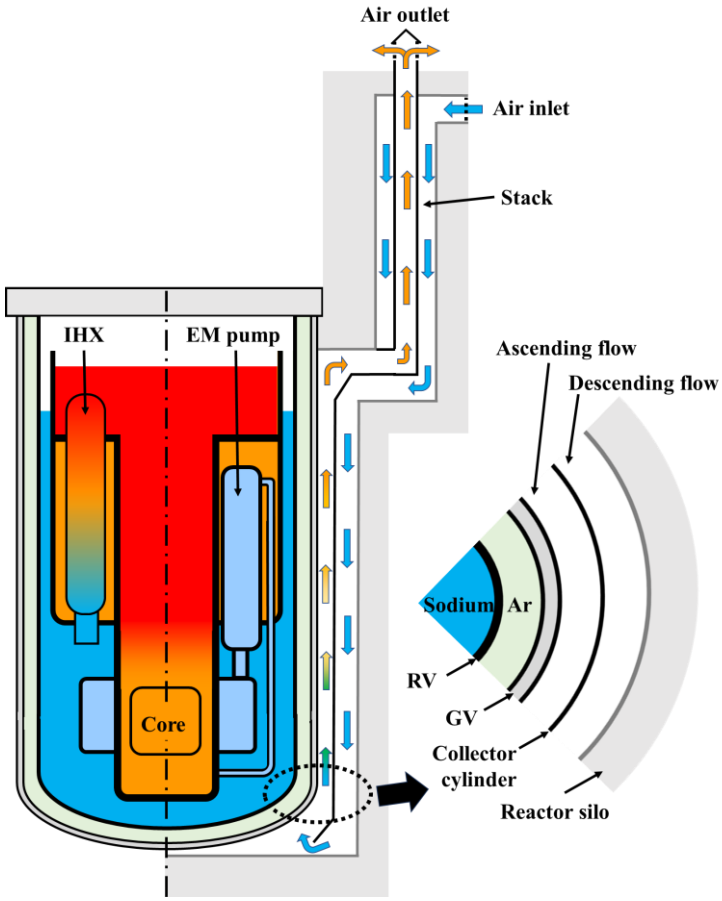

Figure 1. Schematic of RVACS

1.2. Purpose and Approach

During a DBA, the cooling of the core is performed by natural circulation of sodium through reactor scram and the trip of all EM pumps. However, in the event of a primary EM pump failure, which is a representative DBA for SFRs, there is a possibility of backflow of the primary sodium through the failed EM pump. Therefore, it is crucial to confirm the behavior of sodium, especially the transition to natural circulation under the failure condition. Additionally, the method for detecting the failure is important in this case. This is because the EM pump cannot detect its failure with a revolution indicator due to the lack of a drive part, unlike a mechanical pump. Instead, the EM pump power failure is set as the first signal for detecting the failure and immediately triggering a reactor scram. However, the second signal is needed to account for the potential failure of the first signal. Therefore, a preferred physical quantity should be identified for the second signal. Hence, this paper evaluated the behavior of sodium and the effects on RVACS performance in the event of the EM pump failure using a three-dimensional thermal-hydraulic analysis.

2. METHODS

2.1. Model Description

Figure 2 shows the analysis model. This model is based on the specification of a small SFR (reactor thermal power: 471 MWt) with metallic fuel [1], including reactor internal (such as the IHXs, EM pumps, etc.) and the air flow path of the RVACS. This study used the full model with four million cells to deal with an asymentry event, assuming the failure of one of the four EM pumps.

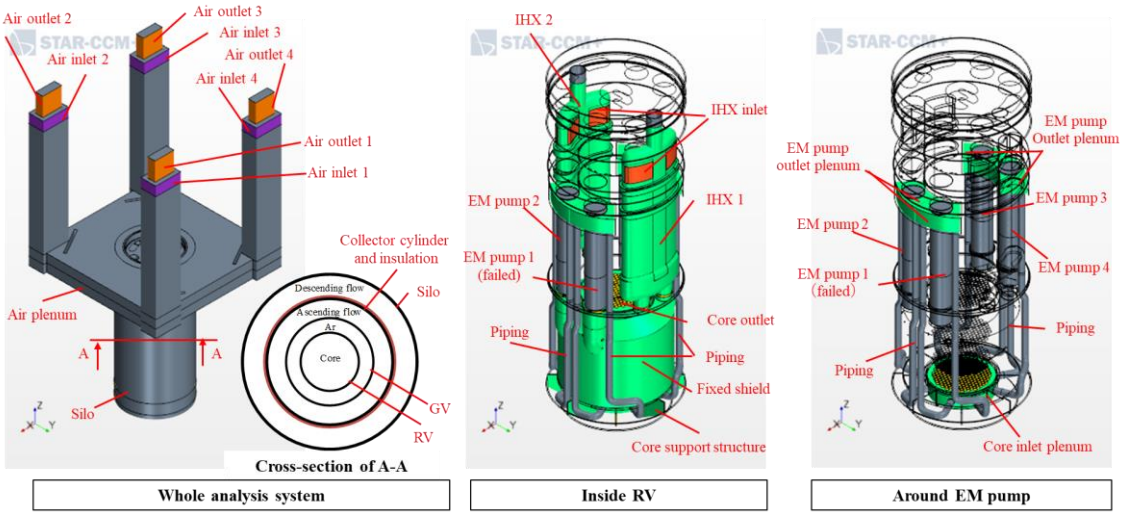

Figure 2. Analysis model

2.2. Model Creation and Validation

The authors created multiple models (one-fourth plane symmetry and full model) for various applications and benchmarked them against U.S. results to evaluate the validity of their analytical methods using STAR-CCM+ ver. 2019.1. First, to verify the analytical method, the authors benchmarked the one-fourth model with three million cells against U.S. results [2]. The intention in creating this model was to establish the analytical method with as few cells and as detailed a model as possible to reduce analysis load. Figure 3 shows the benchmark results against the U.S. results. The plots in this figure show the author's results through reactor scram and the loss of secondary cooling function. As a result, both flow rates decreased with the EM pump driving force, reaching a minimum at 400 s, and finally transitioned to natural circulation. Although the times at which the minimum values were reached differed from the U.S. result, the flow rates after 1000 s were almost consistent with each other. Therefore, the validity of the analytical method was demonstrated.

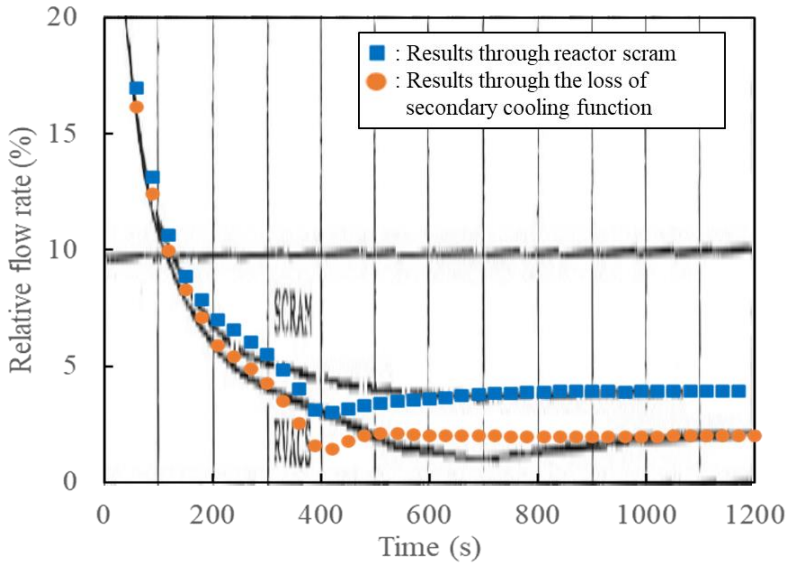

Figure 3. Results of benchmark against the U.S. results*
(* "SCRAM" means the results through reactor scram and the trip of all the EM pumps and "RVACS" means the results through the loss of secondary cooing function.)

Second, two full models with different cells (approximately twelve and four million cells) were benchmarked against the one-fourth model. The former was simply the one-fourth model extended circumferentially, while the latter was a further simplified full model to reduce analysis load. The purpose of this benchmark was to confirm the effects of the simplified model and model asymmetry. Figure 4 shows the benchmark results for the three models. The trends of change in all parameters were very similar, with little relative error (RE). Therefore, the validity of the full model with four million cells used in this study was demonstrated.

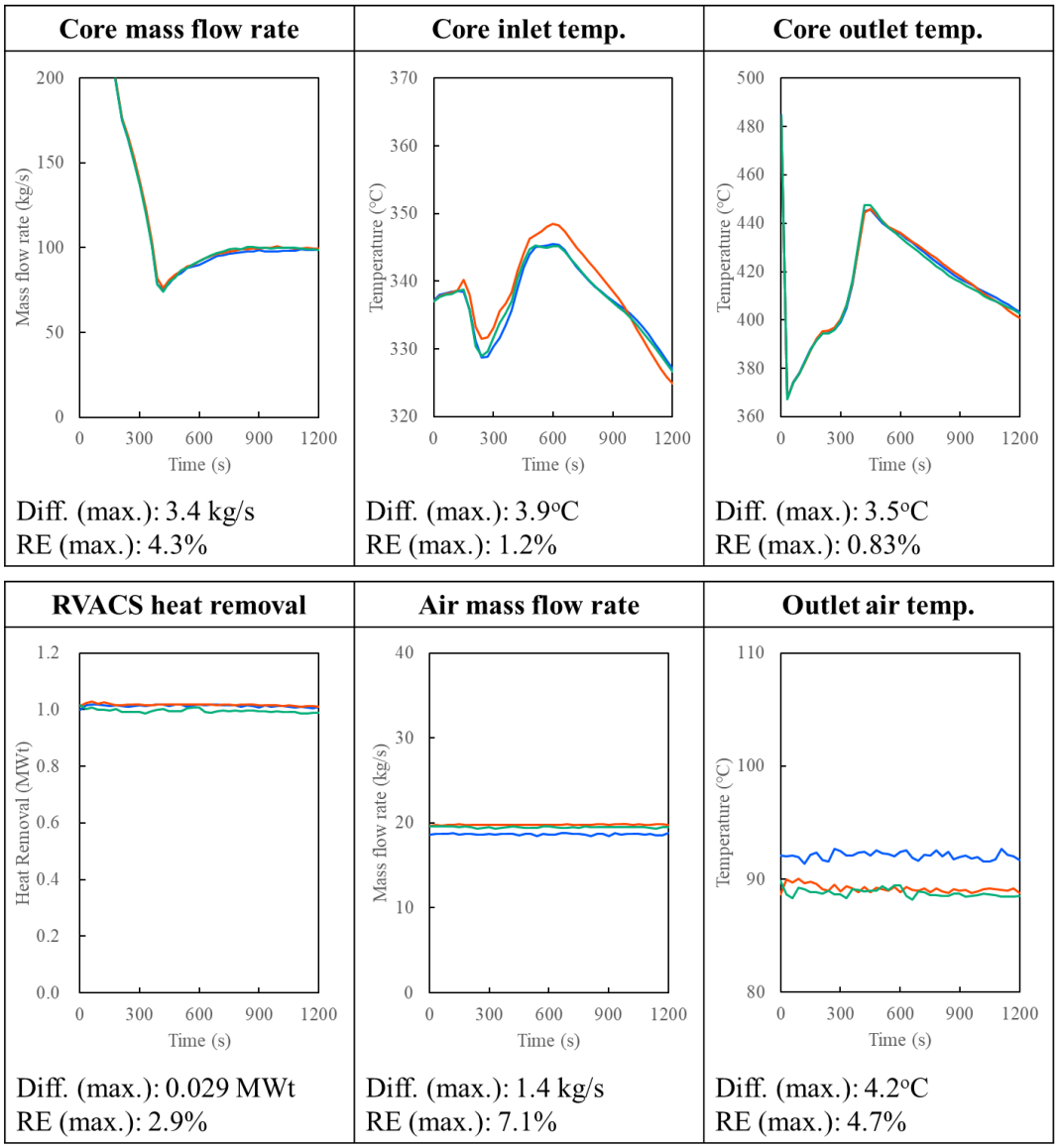

Figure 4. Results of benchmark for the three models
(blue: one-fourth model, red and green: full model with four and twelve million cells)

2.3. Physical Model

This study employs the two-layer realizable *k*-ε turbulence model with the two-layer all y+ wall treatment. The multiband discrete ordinate method was used, and the emissivity of the RV (SS316) and GV (2.25Cr-1Mo) was set to 0.77 and 0.85, respectively. Table 1 shows physical properties used in this study. Since changes in the density of sodium and air affect the driving force of the natural circulation, the density of each was set to depend on temperature based on the ideal gas equation and an approximation calculated from data [3], respectively.

Table 1. Physical Properties
(* all parameters were set as tentative value.)

Parameter	SI Unit	Sodium	Argon	Air	SS316*	2.25Cr-1Mo*	Insulation*	Fuel*
Representative temp.	°C	411	327	67	400	250	20	-
Density	kg/m^3	853	0.811	1.04	7.98×10^3	7.85×10^3	80	1.58×10^4
Specific heat	J/(kg·K)	1.28×10^3	521	1.01×10^3	553	515	1.03×10^3	200
Thermal conductivity	W/(m·K)	70.7	3.05×10^{-2}	2.90×10^{-2}	20.3	32.1	0.03	26.7
Viscosity	Pa·s	2.69×10^{-4}	3.89×10^{-5}	2.06×10^{-5}	-	-	-	-
Reference	-	[3]	[4]	[4]	-	-	-	-

2.4. Boundary Conditions

First, for the boundary conditions on the air flow path side, the air inlet and outlet were set to a stagnant inlet and a pressure outlet, respectively. The air conditions were 38°C and atmospheric pressure. Next, as boundary conditions on the RV side, two scenarios were considered: one in which an EM pump failure was successfully detected, followed by reactor scram and the trip of the remaining EM pumps (Case 1), and the another in which the EM pump failure was not detected, and no operation was performed (Case 2). Case 2 was an open-loop analysis with the following purposes: (1) to confirm whether further events such as primary coolant boiling would occur, and (2) to identify physical quantities that could be detected as the second signal if an emergency reactor shutdown is determined to be necessary.

Figure 5 shows the boundary conditions for Case 1 based on the ANL literature [2]. The events following the EM pump failure were assumed to be as follows:
- 0 s: The head pressure of the failed EM pump was completely lost upon failure.
- 1.0 s: The failure was detected by the first signal.
- 1.2 s: Reactor scram (control rods insertion started).
- 1.3 s: The remaining EM pumps and secondary coolant EM pumps tripped.
- 2.2 s: Control rods insertion completed.

For the boundary conditions of Case 2, the head pressure of the failed EM pumps was only set to 0.

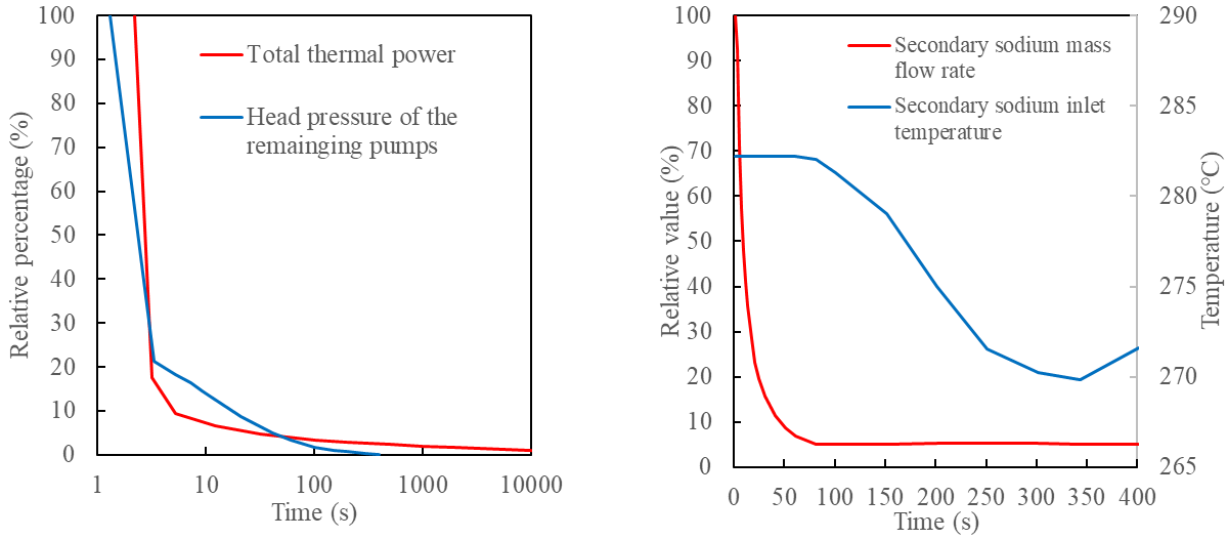

(a) Boundary conditions for primary sodium (b) Boundary conditions for secondary sodium

Figure 5. Boundary Conditions for Case 1
(100% means the rated value during normal operation.)

3. RESULTS AND DISCUSSION

3.1. Case 1 Results

Figure 6 shows the short-term behavior following the failure. As shown in Figure 6(a), backflow began in the failed EM pump, reaching a maximum backflow of 300 %. On the other hand, the flow rate of the remaining EM pumps increased to a maximum of 200%, and the core mass flow rate decreased to 80% until the remaining EM pumps tripped at 1.3s. The core flow rate did not drop significantly because a certain amount of sodium continued to flow from the outlet of the failed EM pump due to fluid inertia. After the EM pumps were tripped, the core outlet temperature rose to a maximum of 520°C as the ratio of thermal power to flow rate increased with a further decrease in the core flow rate. However, the temperature gradually reduced after control rod insertion at 2.2 s as shown in Figure 6(b). Therefore, these results indicated that the core was cooled without sodium boiling in the short period following the failure.

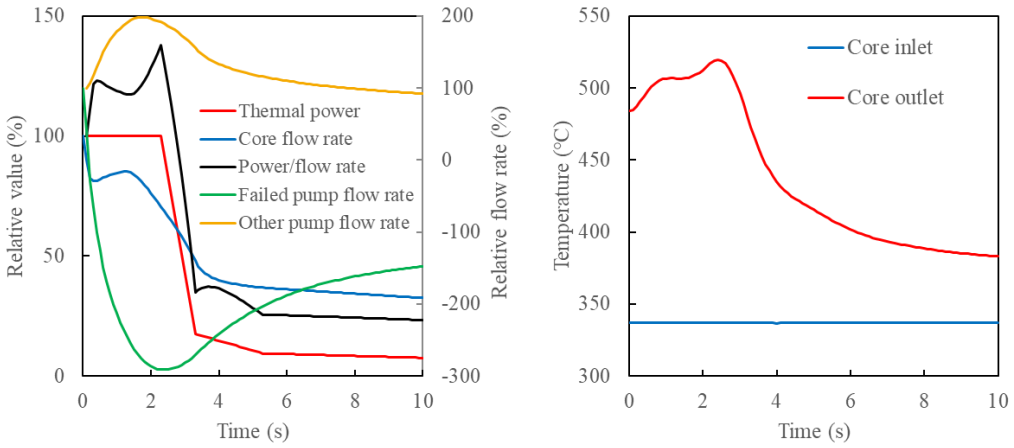

(a) Thermal power and flow rate (b) Core inlet and outlet temperature

Figure 6. Short-term behavior following the failure

Figure 7 shows the behavior from the failure to 1800 s. The dashed lines in these figures represent the transient analysis results through reactor scram, shown in the red line in Figure 4, which provides comparable data for discussing core cooling following the failure. As mentioned earlier, backflow continued in the failed EM pump, but the backflow rate decreased as the flow rate of the remaining EM pumps decreased. The core flow rate decreased due to the EM pump failure and trip, reaching a minimum at 400 s, and then transitioned to natural circulation at 4% flow rate as shown in Figure 7(a). The timing of this minimum coincided with the loss of pump drive power shown in Figure 5(a), and the cessation of discharge from the remaining EM pumps seemed to cause the sodium in the failed EM pump to flow forward. The temperature of the hot and cold pools did not significantly change and the RVACS heat removal also showed a similar trend as shown in Figure 7(b) and 7(c). The small change in heat removal seemed to be due to the large thermal capacity of the RV and GV, resulting in a small change in heat radiation from the GV. Comparison of these results with the transient analysis through reactor scram (dashed line) shows that all changing trends were similar, indicating that stable core cooling was achievable.

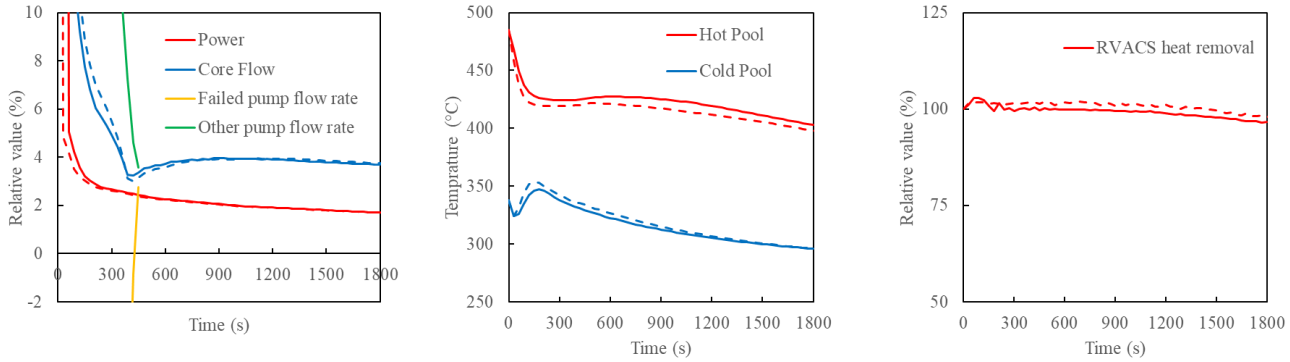

(a) Thermal Power and flow rate (b) Hot and cold pool temperature (c) RVACS heat removal

Figure 7. Behavior from the failure to 1800 s

Figure 8 shows the temperature distribution in the RV. Figure 8(a) shows that although hot sodium remained in the upper part of the hot pool at 120 s, cold sodium flowed into the cold pool over time, forming a low-temperature region, and natural circulation was eventually achieved. Continued heat removal through the IHX may have contributed to the transition to natural circulation. A similar trend was also observed in Figure 8(b).

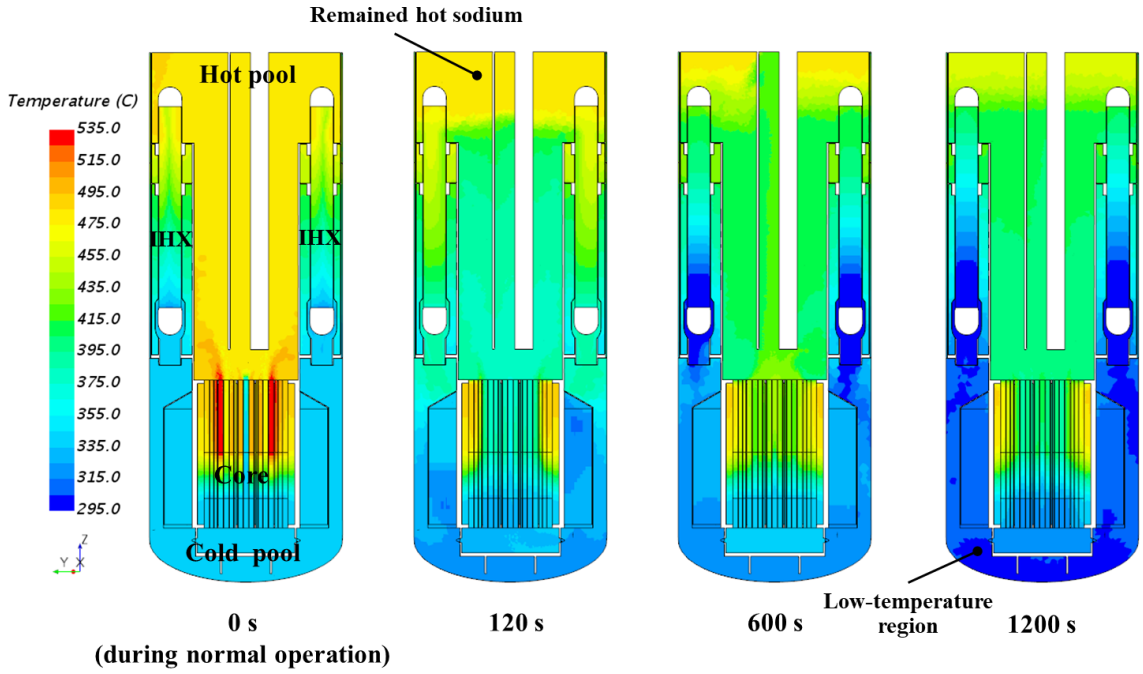

(a) Cross-section of the RV with the IHX

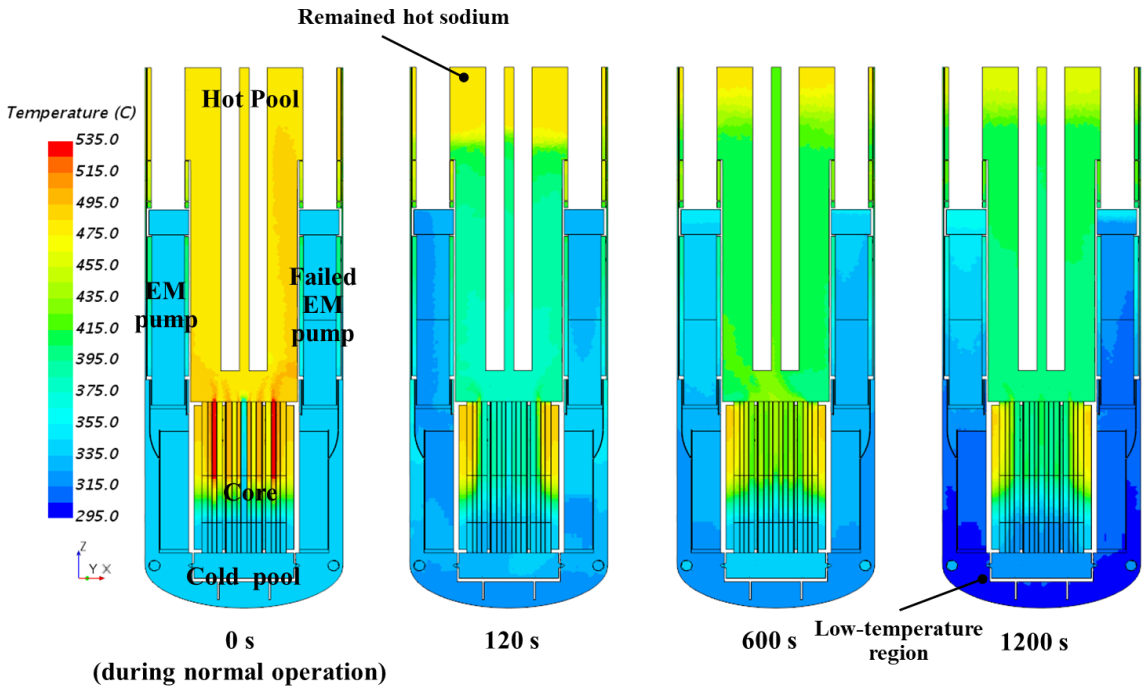

(b) Cross-section of the RV with the failed pump

Figure 8. Temperature distribution in the RV

3.2. Case 2 Results

Figure 9 shows the results of the open-loop analysis, depicting the changes in physical quantities at various location. In the initial seconds following the failure, the outlet pressure of the failed EM pump decreased, and the discharge from the remaining EM pumps initiated backflow into the failed pump. The core outlet temperature rose rapidly as the core flow rate dropped but gradually decreased after reaching a maximum of 508°C. This decrease was due to the relatively stable core flow rate thereafter and the rated heat removal from the IHX, which caused an appropriate drop in the core inlet temperature. This consideration is further supported by the observed decrease in pump outlet temperatures and the core inlet temperature.

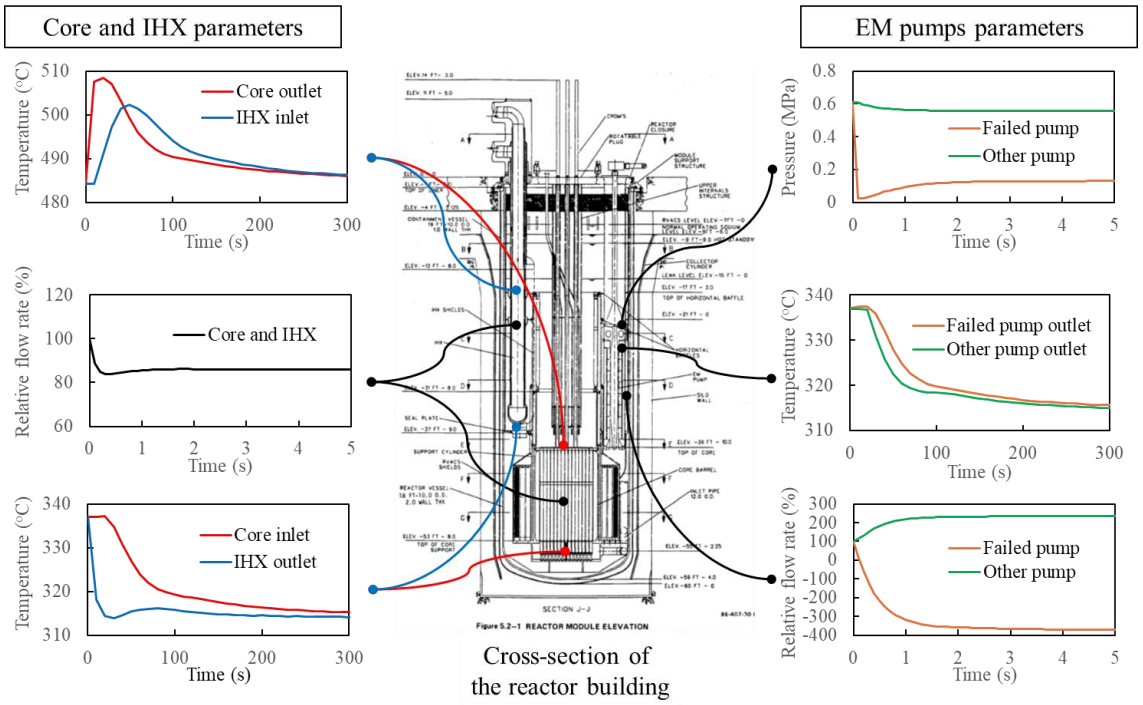

Figure 9. Results of the open-loop analysis

Figure 10 summarizes the event transitions following the failure. Values in parentheses show the amount of variation from the rated value. These results indicate that even without reactor scram following the EM pump failure, the increase in core outlet temperature subsided over time, thereby avoiding sodium boiling. Among the observed changes in physical quantities during the event, the change in pump outlet pressure was the most significant. Therefore, setting pump outlet pressure as the second signal for detecting the failure appears to be desirable. The core outlet temperature could serve as another detection signal, but it may not work well because the thermocouple is covered with a sheath tube, which delays detection, and the core outlet temperature quickly recovers to its original value. Installing an electromagnetic flowmeter in the outlet piping of EM pump could be another detection method, it may be impractical due to the small diameter of the piping.

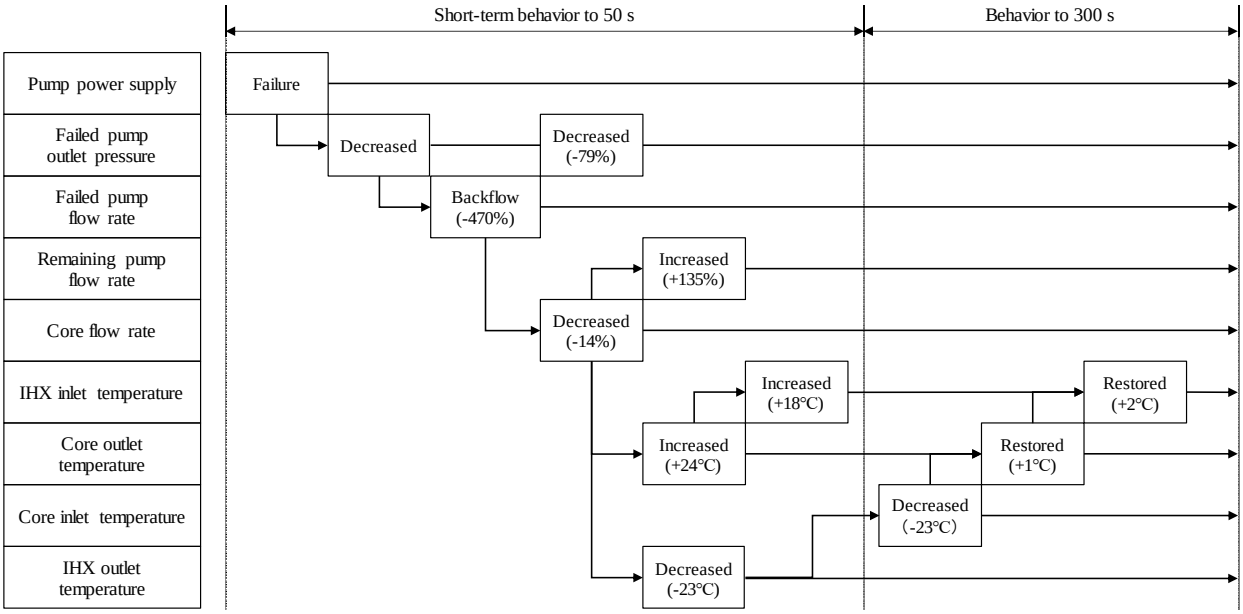

Figure 10. Summary of event transitions following the failure

4. CONCLUSION

This study evaluated the behavior of sodium and the effects on RVACS performance in the event of the EM pump failure using a three-dimensional thermal-hydraulic analysis. The analysis results showed that the primary sodium flowed back in the failed EM pump and the core outlet temperature increased to 520°C as the core flow rate decreased. However, reactor scram and the trip of the remaining EM pumps caused the sodium to shift to natural circulation, with no effects on the RVACS heat removal performance. An open-loop analysis was also performed without reactor scram in the event of EM pump failure to evaluate the variation in each physical quantity. The results of the analysis showed that the core outlet temperature increased due to backflow in the failed EM pump but gradually decreased after reaching a peak due to the stable core flow rate and heat removal from the IHX, confirming that an emergency reactor shutdown was not necessary. Since the largest fluctuation in this analysis was in the pump outlet pressure, setting pump outlet pressure as the second signal for detecting the failure appears to be desirable.

Acknowledge

This research used resources of the Program to Support the Development of Innovative Nuclear Power Technologies in Response to Society's Needs of the Ministry of Economy, Trade, and Industry.

References

[1] General Electric. PRISM Preliminary Safety Information Document. GEFR-00793, 1967.
[2] P. L. Garner. Thermal-Hydraulic Analysis of Scram and RVACS Transients in PRISM Using COMMIX-1AR: Short Term Response. ANL-PRISM-38, 1987.
[3] G. H. Golden. Thermophysical Properties of Sodium. ANL-7323, 1967.
[4] JSME Data Book: Heat Transfer 4th Edition, 1986.